AJNR

Functional MR Imaging Using a Visually Guided Saccade Paradigm for Comparing Activation Patterns in Patients with Probable Alzheimer's Disease and in Cognitively Able Elderly Volunteers

Keith R. Thulborn, Claudine Martin and James T. Voyvodic

AJNR Am J Neuroradiol 2000, 21 (3) 524-531
http://www.ajnr.org/content/21/3/524

AJNR Am J Neuroradiol 21:524–531, March 2000

Functional MR Imaging Using a Visually Guided Saccade Paradigm for Comparing Activation Patterns in Patients with Probable Alzheimer's Disease and in Cognitively Able Elderly Volunteers

Keith R. Thulborn, Claudine Martin, and James T. Voyvodic

BACKGROUND AND PURPOSE: **Alzheimer's disease is associated with progressive visuospatial dysfunction. This study used functional MR (fMR) imaging with an eye movement paradigm to investigate differences in visuospatial cognition between patients with probable Alzheimer's disease (pAD) and cognitively able elderly volunteers.**

METHODS: **Using established, although imperfect, clinical criteria, patients with pAD (n = 18) and cognitively able elderly volunteers (n = 10) were selected for study. All patients underwent echo-planar fMR imaging at 1.5 T. The visually guided saccade paradigm consisted of alternating periods (30 s) of central fixation and visually guided saccades to a target appearing randomly along the horizontal meridian. Activation maps were derived using a voxelwise *t* test, comparing the signal intensities between the two steady-state conditions. The activation patterns were characterized by Talairach coordinates, activation volumes, and laterality ratios (LRs).**

RESULTS: **Statistically significant differences existed between the activation patterns of the patients with pAD and those of the volunteers. In contrast to the control group, a left-dominant parietal activation pattern and enhanced prefrontal cortical activation were observed in most patients with pAD.**

CONCLUSION: **Within the limitations of the imperfect clinical standard of reference, the reduction in right parietal activation producing the left-dominant LR for the intraparietal sulcus may reflect the progressive dysfunction in spatial attention associated with Alzheimer's disease, considering the known parietal lobe involvement in this function and the disease. The high specificity of a positive intraparietal sulcal LR measured by fMR imaging may have a role in detecting and monitoring Alzheimer's disease.**

Poor visuospatial skills, rather than problems with the retina or optic nerves, underlie the visual complaints that are commonly expressed by patients with probable Alzheimer's disease (pAD) (1–4). Limited attention shifting and hemifield neglect are possible explanations for these visual dysfunctions (5, 6). These results have been reported by neuropsychological testing (1, 4–7) and positron emission tomography (PET) of cerebral blood flow (3, 8) and have been attributed to dysfunction of the associative visual cortex in the parietal lobes. Specifically, left hemifield neglect, which is present in a significant portion of patients with pAD (6), is linked to lesions in the right parietal lobe (9–11). More recently, PET and functional MR (fMR) imaging studies have revealed the role of right and left parietal lobes in spatial and temporal visual attention, respectively, in cognitively able volunteers (12). Considering that the neurofibrillary tangles and amyloid plaques that characterize pAD are found predominantly in the associative cortex rather than in the primary visual occipital cortex, it is perhaps not surprising that visuospatial processing is abnormal.

Although the diagnosis of Alzheimer's disease is confirmed definitively only at autopsy or, less commonly, by biopsy, extensive neuropsychological and psychiatric evaluations over time can provide the diagnosis of pAD while the patient is alive. The

Received April 19, 1999; accepted after revision October 22.

From the Department of Radiology, MR Research Center, University of Pittsburgh Medical Center, Pittsburgh, PA.

This work was presented in preliminary form at the 1998 Annual Meeting of the Society for Neuroscience and at the 1999 Annual Meeting of the American Society of Neuroradiology.

Address reprint requests to Keith R. Thulborn, MD, PhD, MR Research Center, B855, Presbyterian University Hospital, 200 Lothrop Street, Pittsburgh PA 15213–2582.

detection of pAD in the early stages of the disease remains a challenge.

The guidelines for the clinical diagnosis of pAD are the outcome of a consensus conference chaired by McKann in 1984 (13) for the organization that was once called the National Institute for Neurological and Communicative Disorders and the Alzheimer's Disease and Related Disorders Association. Although this organization has been divided into separate institutes within the National Institutes of Health (Bethseda, MD) and the Alzheimer's Association (Chicago, IL), the clinical criteria remain unchanged. The sensitivity and specificity of clinical criteria for pAD have not been formally assigned, but an accumulated experience has been obtained. Typically, the sensitivity of the initial clinical diagnosis of pAD after neurologic, psychological, and psychiatric examinations is high (>90%), which is not unexpected considering the high incidence of this type of dementia in the elderly. The specificity is much lower (<70%) based on confirmed autopsy diagnoses. Both sensitivity and specificity improve, as determined by follow-up over the course of the disease, although specificity (~80%) never approaches sensitivity (>95%) (DeKosky S, Becker J, and Lopez O; Alzheimer's Disease Research Center, University of Pittsburgh; personal communication).

Visuospatial skill testing has been advocated as contributing to the diagnostic procedure (4), although it was not used in the clinical studies described herein for which sensitivity and specificity have been derived. An interesting approach using PET as the method of neuroimaging was proposed to investigate the compensatory changes in the right hemispheric ventral neural network with a face-matching task that may precede any overt decline in behavioral performance (14). Similarly, a functional neuroimaging study of a task involving the parietal lobes may reveal such dysfunction, thereby aiding diagnosis and possibly providing a more sensitive quantitative means of following regional effects of potentially therapeutic drugs than what neuropsychological testing provides.

Although fMR imaging has been used to map patterns of many different large-scale neurocognitive networks in cognitively able volunteers, application of this methodology to patient populations is in its infancy (15–21). Because blood oxygenation level–dependent (BOLD) fMR imaging (22, 23) depends on a regional hemodynamic response from increased neuronal activity, changes in the underlying cerebrovascular functions and measurements must be considered in patient studies.

In cases of early pAD, single-photon emission CT has documented perfusion abnormalities in the parietal lobes bilaterally that correlated with cognitive performance on visual perception tasks (24). Visual perception requiring semantic and lexical knowledge has been reported as showing early and progressive deficiency in pAD (25). Because most patients with dementia undergo MR imaging as a part of their clinical evaluation for treatable causes, the challenges of fMR imaging faced with the evaluation of dementia are worth addressing. Patient cooperation in performing the cognitive paradigm while minimizing head motion is of particular importance in fMR imaging. This novel environment adds cognitive demands for patients with dementia by requiring attention to the paradigm yet also requiring that the patient ignore acoustic stimuli from the imager. Instructions regarding how to perform the task, as well as the cognitive task itself, must be matched to the reduced cognitive capabilities of the patient with dementia.

We have chosen a very simple reflexive eye movement paradigm based on visually guided saccades for which considerable behavioral data has been obtained from cognitively able human volunteers as well as electrophysiologic data derived from non-human primates without neurologic deficit. Functional MR imaging studies of this paradigm in cognitively able adults have consistently shown robust activation of a large-scale neurocognitive network that includes the parietal cortex (14, 25, 26).

We have compared the activation patterns from fMR imaging of the dorsal cerebral cortex by using a visually guided saccade paradigm in cognitively able elderly control subjects and patients with pAD. This study was designed to test whether significantly different activation patterns were associated with the parietal regions that may reflect the known parietal lobe involvement of Alzheimer's dementia.

Methods

Patients undergoing evaluation of dementia for pAD were referred for conventional MR examination to exclude underlying structural pathologic abnormalities. Patients capable of performing the visually guided saccades paradigm, as evidenced by their performance on the task on a computer display at the time of the routine MR screening interview, were asked if they would like to participate in the fMR imaging study. All such patients or their guardians provided informed written consent as approved by our institutional review board. Because imaging was performed before diagnosis was made, only 18 of a total of 24 patients with successful fMR imaging studies were diagnosed as having pAD after the initial evaluation and after at least 1 year of clinical follow-up evaluations were completed. This evaluation included extensive medical, neuropsychological, and psychiatric evaluation. A consensus diagnosis involving discussions between neurologist, psychiatrist, and neuropsychologist was obtained for each patient. All patients diagnosed with pAD met the criteria of the National Institute of Neurological and Communicative Disorders and Stroke (National Institutes of Health; Bethseda, MD) and the Alzheimer's Association (Chicago, IL) for the disease (13). This group included pAD without and with atypical presentation, atypical course, or extrapyramidal features (n = 18; male:female ratio, 8:10; mean age [male], 74 ± 6 years; mean age [female], 73 ± 9 years; age range, 61–90 years; mini-mental status [male subjects], score of 15.6 ± 4.1; mini-mental status [female subjects], score of 18.7 ± 5.6). All patients were right-handed except for two, one of whom was left-handed and one of whom was ambidextrous. The overall failure rate for fMR imaging studies performed for this group was 44% over 3 years from our initial studies to current practice.

The group of patients being evaluated for pAD who did not meet these criteria after at least 1 year of follow-up included other dementia (n = 2) and non-dementia (n = 4) categories (n = 6; all female subjects; mean age, 65 ± 10 years; age range, 49–72 years; mini-mental status, score of 24.8 ± 5.0; score range, 18–30; all right-handed). These patients were evaluated in identical fashion clinically and with imaging. The overall technical failure rate based on fMR imaging studies performed for this group was 50%. Because this group was heterogeneous but achieved results similar to those of the control group, this group is not included in this report.

Cognitively able elderly volunteers (n = 10; male:female ratio, 3:7; age range, 70–89 years; all right-handed) were recruited from other studies requiring such control participants and were selected based on a negative psychiatric history and a willingness to participate in this study. This group had a technical failure rate of approximately 50%.

The visually guided saccade paradigm has been described in detail (14, 26, 27). Briefly, the visually guided saccade paradigm consisted of multiple cycles of alternating central fixation on a small cross (<0.75°) (30 s) with a spot of light (1.0°) that randomly appeared at one of five positions (separation of 3°) along the horizontal meridian (30 s). The number of cycles was 6.5 for studies performed with seven image sections and 10.5 for studies with 14 image sections. This difference was used to produce comparable numbers of images in the statistical analysis with increased brain coverage at a fixed imager duty cycle.

Technically inadequate fMR imaging studies obtained using the visually guided saccade paradigm across all studies in this elderly patient and control population were largely caused by excessive head motion and showed no differences in distribution of gender, age, or diagnosis from the successful studies. When the first studies were attempted, the success rate was low, but as we gained experience with explaining and demonstrating the study to the volunteers, the technical success rate increased to more than 70%.

MR imaging was performed on a 1.5-T whole-body imager equipped with resonant-gradient echo-planar imaging and data-handling capabilities designed for fMR imaging as previously described (14, 17, 19). The commercial quadrature birdcage head coil was used. Each patient was placed in a comfortable, supine position with light padding around the head within the RF coil. Subjects were able to see a rear-projection screen suspended inside the magnet bore via the angled mirror of the commercial head coil. The visual stimuli were projected onto this screen. Subjects wore ear plugs to reduce their perception of acoustic noise caused by switching gradients during echo-planar imaging. Because no MR-compatible eye tracking system was available when this investigation was performed, eye movement was not monitored during the imaging session.

The functional images were acquired as a time series of either 260 or 210 images, using a fat-saturated, gradient-echo, echo-planar acquisition scheme. The imaging parameters, optimized for BOLD contrast, were as follows: 1500 or 3000 (TR) for seven or 14 axial sections, respectively/50 (TE); flip angle, 90°; acquisition matrix, 128 × 64; field of view, 40 × 20 cm^2; section thickness, 5 mm; and section gap, 1 mm.

The structural images were acquired with a 3D, gradient-echo sequence (spoiled gradient-recalled acquisition in the steady state; 25/5; field of view, 24 × 18 cm^2; matrix, 256 × 192; flip angle, 40°; section thickness, 1.5 mm; no gap). Conventional series of images were also acquired as a part of the clinical MR evaluation, but because they are not part of this study, no further description is relevant.

The fMR imaging data were analyzed in three stages, and those interpreting the images were blinded to diagnosis. Data were inspected for excessive motion by visualization in an animation loop, and motion was quantified using image registration software described elsewhere (28). Data sets with greater than one voxel of in-plane motion across the duration of the paradigm were excluded from further analysis. Image reregistration was not performed because correction methods for 3D motion require 3D image acquisitions for reliable correction; these data were acquired in a multisection mode. Once suitable data sets were selected, a voxel-wise Student's *t* test was used to compare the signal intensity of active and fixation conditions across the paradigm, as described elsewhere (14–16). The activation maps of individual participants were examined over a range of *t* thresholds ($2.5 < t < 5.5$) encompassing from 1.3 ± 0.6% (upper *t* value) to 5.0 ± 1.8% (lower *t* value) of the total number of voxels (mean ± SD) in the seven images. Only seven sections were used from the 14 section acquisitions. This introduced no biases between the analyses of the seven and 14 section studies from the image quality as judged by comparable signal-to-noise ratios for both types of acquisition. This approach ensured that results were not biased by the choice of *t* threshold and that bias toward the participants with high levels of activation was avoided. The activation map of each patient was superimposed onto that person's own structural images.

Using AFNI software (29) and after transformation into Talairach coordinate space (30), the regions of peak activation (highest *t* value) were recorded by the Talairach coordinates and Brodmann areas. The SD of the average coordinates of all individual patients in a group gave a measure of biological variance in localization that was not shown from a group activation map of Talairach transformed images accumulated with the AFNI software. The numbers of active voxels above a set of specified *t* values ($2.5 \leq t \leq 5.5$) over the dorsal cortex covered by the seven most superior sections common to all studies were counted manually for the four active regions of each cerebral hemisphere for each patient. These four regions in each cerebral hemisphere were the frontal eye field (FEF, along the precentral sulcus), supplementary eye field (SEF, along the medial frontal lobe), intraparietal sulcus (IPS, along the intraparietal sulcus), and prefrontal cortex (PFC, anterior to the prefrontal sulcus in the middle frontal gyrus). The percent MR signal change between the fixation and saccade conditions was determined for the voxel at the peak *t* value within each region of each participant in each group. The mean and SD of these MR signal change percentages for each area were calculated for each group.

The distribution of activation across each of these areas was characterized as the percentage of the total active volume. This percent active volume was defined rAV/tAV, where rAV signifies the number of active voxels in each area and tAV signifies total active voxels in all four regions of both hemispheres. Using AFNI software, group activation patterns were generated in the common coordinate space of Talairach by the superposition of the activation maps of individual participants over the group structural maps. Both individual and group patterns were examined for statistically significant hemispheric differences using a two-tailed paired *t* test. Differences between groups were investigated by two-tailed unpaired *t* tests.

The laterality ratio (LR) was defined as the ratio of the difference in the number of activated voxels in the left and right hemispheres to the sum of the number of activated voxels in the left and right hemispheres, such that $LR(X) = (L - R)/(L + R)$, where L and R are the number of activated voxels in area X (FEF, SEF, IPS, PFC) of the left and right hemispheres, respectively. LRs for the IPS were calculated for all participants over the range of *t* thresholds counted, as described previously in this Methods section, and examined for each group to show the spread of this parameter across participants, *t* values, and groups.

The volume measurements of cerebral hemispheres, occipitoparietal lobes, and ventricles were made using custom-designed segmentation software, MORPH, which has been presented previously (31). This used a mixture-modeling algorithm to determine objectively the border of selected structures with high image contrast and thereby calculate a volume.

TABLE 1: Activation data for individual control subjects (n = 10, mean and SD) tabulated as Talairach coordinates, Brodmann areas, and % signal change for activation peaks in regions of supplementary eye fields (SEF), frontal eye fields (FEF), prefrontal cortex (PFC), and intraparietal sulcus (IPS) for the left and right hemispheres for the visually guided saccade paradigm

		Left Hemisphere				Right Hemisphere			
Region	Brodmann Area	*x* (mm)	*y* (mm)	*z* (mm)	% Signal Change	*x* (mm)	*y* (mm)	*z* (mm)	% Signal Change
SEF	6	−5 ± 2	−6 ± 7	56 ± 7	0.5 ± 0.5	4 ± 3	−4 ± 8	57 ± 6	0.9 ± 0.6
FEF	6/8	−35 ± 9	−11 ± 5	48 ± 4	1.0 ± 0.4	33 ± 10	−8 ± 8	48 ± 3	1.3 ± 1.0
PFC	9	−34 ± 9	35 ± 5	35 ± 3	0.5 ± 0.3	30 ± 6	36 ± 12	33 ± 5	0.7 ± 0.3
IPS	19	−26 ± 10	−73 ± 9	33 ± 9	1.0 ± 0.6	24 ± 10	−70 ± 12	35 ± 10	0.9 ± 0.6

TABLE 2: Activation data for individual subjects with probable Alzheimer's disease (n = 15, mean and SD) tabulated as Talairach coordinates, Brodmann areas, and % signal change for activation peaks in regions of SEF, FEF, PFC, and IPS as in Table 1

		Left Hemisphere				Right Hemisphere			
Regions	Brodmann Area	*x* (mm)	*y* (mm)	*z* (mm)	% Signal Change	*x* (mm)	*y* (mm)	*z* (mm)	% Signal Change
SEF	6	−4 ± 1	−11 ± 7	59 ± 7	1.1 ± 0.9	2 ± 2	−9 ± 9	59 ± 7	0.8 ± 0.5
FEF	6/8	−35 ± 9	−12 ± 6	50 ± 6	0.9 ± 0.5	31 ± 8	−13 ± 8	50 ± 7	0.7 ± 0.4
PFC	9	−38 ± 7	28 ± 7	31 ± 5	0.8 ± 0.5	32 ± 6	36 ± 8	33 ± 7	0.8 ± 0.5
IPS	7	−26 ± 8	−65 ± 10	45 ± 5	0.9 ± 0.5	27 ± 7	−62 ± 9	46 ± 7	0.9 ± 0.7

Note.—The coordinates for three of 18 patients were not obtained as the high-resolution images were not available.

The occipitoparietal volumes were measured on the high-resolution coronal images from the medial aspect of the central sulcus posterior to the occipital pole. Volumes were compared between groups by an unpaired *t* test.

Results

The mean Talairach coordinates, Brodmann areas, and peak percent signal change of the four regions of activation (FEF, SEF, IPS, PFC) are presented in Table 1 for each hemisphere of the individual data for the cognitively able elderly group. The equivalent results for the patients with pAD are presented in Table 2. The variation in coordinates determined for each epicenter of activation of each individual was less than 15 mm for both groups. The group activation maps also gave activation epicenter coordinates (not shown) within the same variance as averaging individual participant coordinates for each group (Tables 1 and 2). There was little difference in the SD of the coordinates across the individual participants of both groups for the four areas. A wider spread of activation around the PFC epicenter was observed on the activation map of the pAD group than on the activation map of the control volunteers, as shown in Figure 1. The signal change for BOLD contrast of approximately 1% did not vary between hemispheres of individual participants or between the two groups (Tables 1 and 2). The measurements of total parenchymal volumes of the cerebral hemispheres were not significantly different between the two groups (control group, 869 ± 101 cm^3; pAD group, 831 ± 113 cm^3). Similarly, no differences were found for the smaller regions, such as the occipitoparietal region.

Figure 1 shows activation maps in seven axial planes for the pAD and control groups (panels *A* and *B*, respectively). The distributions of activation for the pAD and control groups are summarized in Figure 2 (panels *A* and *B*, respectively) as plots of a percentage activation volume in right and left hemispheres for each of the four sites of activation (SEF, FEF, IPS, PFC). This percentage distribution parameter effectively normalizes the amount of activation, independent of the chosen *t* threshold, to allow the patterns in the two groups to be compared. LRs for both groups are presented in Table 3.

There were statistically significant differences in activation between areas in the cerebral hemispheres within and between the groups. The IPS activation showed right-hemisphere dominance (negative LR) in the elderly control group. This result reversed to a left-hemisphere dominance (positive LR) for the pAD group. The resultant, significantly altered IPS LR arose from the reduced percentage of activation volume in the right IPS for the pAD group. No statistically significant differences were found in other areas between groups.

No significant correlation (coefficient = 0.4) was found between mini-mental status scores and the LR of IPS or PFC or for frontoparietal activation ratios for individual participants. Although Figure 2 emphasizes the group differences between the pAD and control groups, Figure 3 shows the distribution of activation volumes between the right and left hemispheres for individual participants within each group. Although most patients with pAD showed reversal of the right-dominant IPS activation of the control group, six of 18 patients

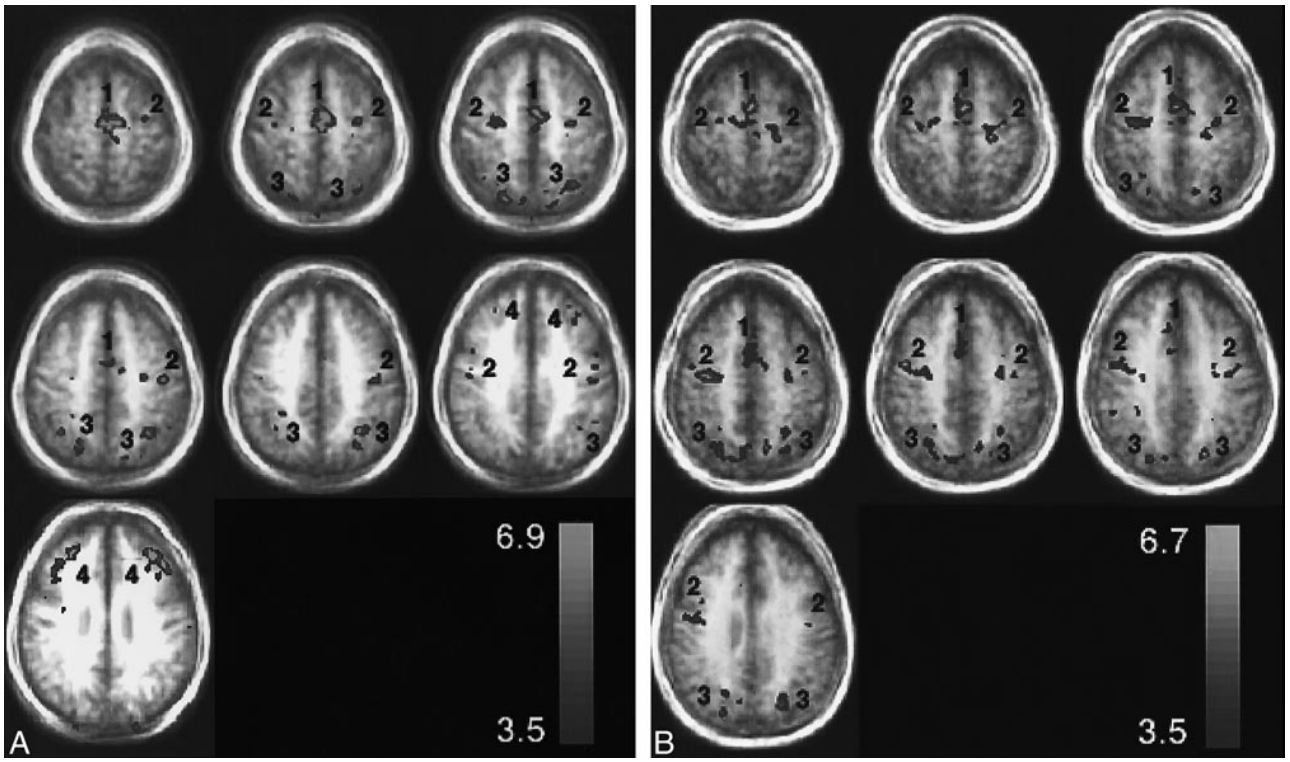

FIG 1. Representative group axial activation maps ($t > 3.5$) for the visually guided saccade paradigm through the SEF (*1*), FEF (*2*), IPS (*3*), and PFC (*4*). The activation is displayed as a hot iron color scale (*bottom right*) where *red* is the lowest *t* threshold and *yellow* is the peak *t* value. The activation is displayed over group structural images to show the degree of blurring from biological anatomic variation. *A* relates to patients with pAD and *B* to control volunteers.

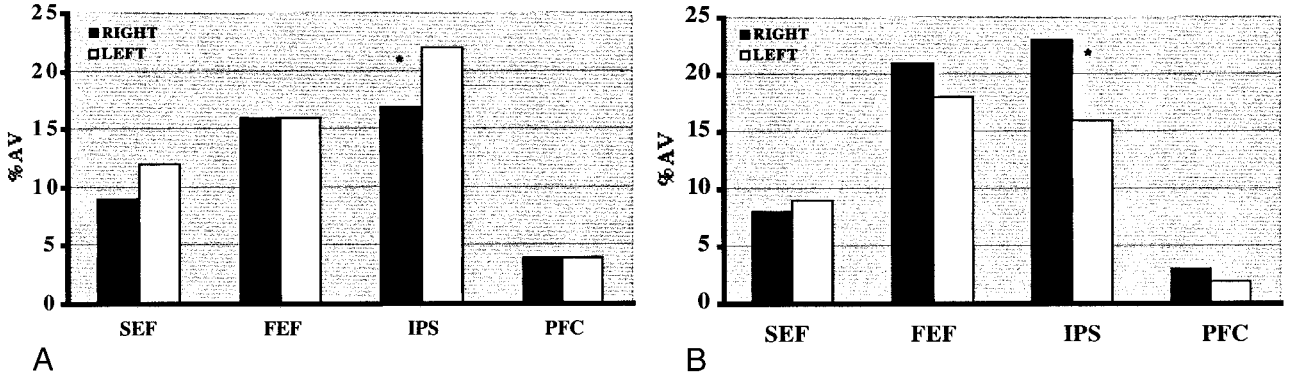

FIG 2. Percent activation volume in each of four areas of activation in right and left cerebral hemispheres for the visually guided saccade paradigm. The regions are SEF, FEF, IPS, and PFC. The voxel numbers for each region were pooled from the activation maps of each participant. Table 3 shows that there is a corresponding significant difference ($P < .02$, unpaired two-tail *t* test) in LR for IPS between the normal group and the pAD group.

A, pAD group (n = 18). *, statistically significant difference ($P < .10$, paired two-tailed *t* test) between the volume of activation for the right and left hemispheres.

B, Control group (n = 10). *, statistically significant difference ($P < .001$, paired two-tailed *t* test) between the volume of activation for the right and left hemispheres.

(33%) showed the pattern of the control group. This effect is seen in Figure 4, which shows the right and left hemispheric components of the IPS LR for individuals in each group. Although all individuals in the control group clustered below an IPS laterality threshold (LR[IPS] < 0.02), the pAD group showed a greater spread. Such separation was not observed for the other regions of interest (SEF, FEF, PFC).

Discussion

When appropriate care is taken for quality assurance of instrumentation (19) and preparation of participants (16, 17), fMR imaging is a robust method for studying brain function in cognitively able volunteers (14). The elderly patient with dementia represents a challenge for fMR imaging because of the high level of cooperation required and the need for paradigms to be appropriate to the cog-

TABLE 3: Mean LRs for the four regions of interest defined in Table 1 for the pAD and elderly control groups

Region of Interest	LR(pAD) (n = 18)	LR(Controls) (n = 10)
SEF*	0.15 ± 0.22	0.11 ± 0.29
FEF	−0.01 ± 0.30	−0.05 ± 0.28
PFC	−0.22 ± 0.53	−0.36 ± 0.52
IPS**	0.10 ± 0.34	−0.18 ± 0.11***

Note.—LRs are calculated for each individual and averaged over the group to define an SD for each group.

* The LR(SEF) was significantly non-zero for the pAD group (two-tailed, paired *t*-test, $P < .02$) but not so for the control group (two-tailed, paired *t*-test, $P < .16$).

** The LR(IPS) was significantly non zero, ie, asymmetrical, for the control group (two-tailed, paired *t*-test, $P < .001$) but not so for the pAD group (two-tailed, paired *t*-test, $P < .10$).

*** Statistically significant difference (two-tailed, unpaired *t*-test, $P < .02$) between control and pAD groups.

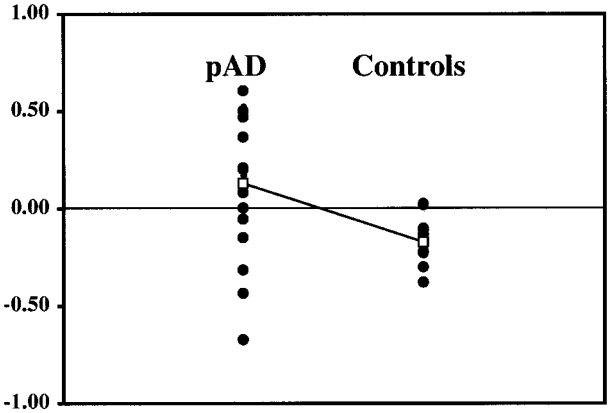

FIG 3. LR for IPS of individual participants ● of the pAD and control groups. The mean LR □ for each group was significantly different ($P < .02$, unpaired two-tailed *t* test). The other regions of interest (PFC, SEF, FEF) did not show significant separations (not shown).

nitive performance of this population. Our technical success rate, although initially low, improved with increased patient training time (always shorter than 10 min), more comfortable positioning, and reduced duration of the paradigm and by performing fMR imaging immediately after instruction rather than after the conventional anatomic MR examination. The same nursing and technologist staff accumulated this experience during a 3-year interval.

One limitation of this fMR imaging study is the lack of a measure of task performance during imaging that could be used for correlation with activation. As group data were used, however, activation patterns showed common areas of activation for both patient and control groups. Only those patients who were able to perform this simple reflexive eye movement task outside the imager were tested in the imager. This limitation is therefore unlikely to influence the general interpretation of the data presented.

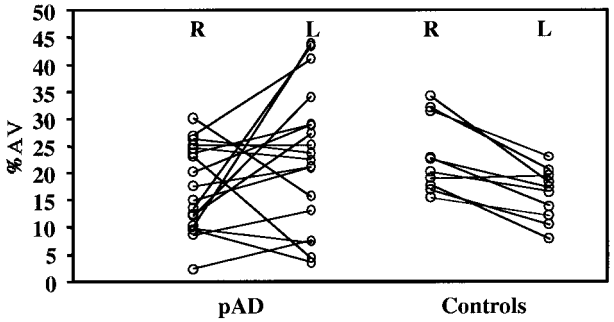

FIG 4. Percent activation volume for the IPS regions of the right (*R*) and left (*L*) hemispheres of individual participants in the pAD and control groups, showing the group mean values. Right and left values are connected for each participant to show both individual trends within each group.

Another limitation of this study is the use of the clinical diagnosis as a standard of reference despite its known low specificity. The use of a more definitive standard, such as biopsy and autopsy proof of diagnosis, was not possible for this report. The high sensitivity of the clinical diagnosis, however, implies a low false-negative rate. Note that, using the fMR imaging criterion of IPS(IPS) > 0.02, patients without pAD and control subjects were not falsely diagnosed as having pAD. The high sensitivity of the clinical criteria was expected to produce some heterogeneity with false-positive diagnoses in the pAD group. Again, the IPS LR also showed greater variability for this pAD group. Whether patients classified clinically as having pAD with LR below 0.02 will eventually be reclassified based on follow-up and ultimately autopsy examinations cannot yet be determined. Considering the imperfect clinical criteria, the current results support the usefulness of an IPS LR greater than 0.02 as an indicator of pAD (specificity = 100%, sensitivity = 66%).

Although the group activation patterns visually summarize the different distributions of activation over a dorsal activation pathway for eye movement control in the control and pAD groups, the group data were not essential for this result. As shown in Figure 4, the activation maps from individual patients with pAD could be grouped by visual inspection into two subgroups of LR(IPS) ≥ 0.02 and LR(IPS) < 0.02. The LR(IPS) ≥ 0.02 was diagnostic of pAD with a specificity of 100%, although at a lower sensitivity of 66%. Although control volunteers showed right-dominant parietal activation and low prefrontal cortical activation, patients with pAD had less right than left parietal activation and increased prefrontal activation. In contrast to elderly groups, normal young adults seldom show PFC activation, although parietal activation remains right-hemisphere dominant (27). The variation in LR was not explained by gender differences within and between groups. The low number of participants in gender subgroups reduced the power of this result, but gender differences were also not reported with this paradigm in other studies of control volunteers (27).

Because global measurements of the cerebral hemispheres and local measurements of the occipitoparietal lobes showed no volumetric differences between the control and pAD groups, it is unlikely that the observed differences in activation patterns can be attributed to morphometric differences between the groups. Because the peak signal changes for BOLD contrast were comparable for all areas and groups, it is unlikely that differences in the mechanism of BOLD contrast can explain the observed differences between areas or groups.

A general concern regarding the statistical nature of activation maps obtained with fMR imaging is the choice of the threshold for statistical significance. When a *t* test is used, a result obtained at some arbitrary *t* threshold may be questioned for robustness across other thresholds. This potential concern has been addressed in this study by examining all data over a range of *t* thresholds. In this case, the range examined encompassed from 1% to 5% of the most active voxels or *t* values between 2.5 and 5.5. The results are robust over this range (ie, independent of *t* threshold). Higher *t* thresholds ($t > 5.5$) provide fewer than five voxels per area and make calculation of LRs unreliable. Lower *t* thresholds ($t < 2.5$) show apparent activation distributed randomly over the brain. Thus, the range used in this study is appropriate for the sensitivity of a BOLD contrast fMR imaging study at 1.5 T in these populations. Increased sensitivity at a higher field strength may be a useful means to evaluate these results further (19, 20).

The different patterns of activation in the two population groups can be rationalized using a model of cognitive function reported previously on cognitively able volunteers performing language comprehension (32) and visuospatial processing (33) tasks of increasing difficulty. As the degree of difficulty of the task was increased, the volume of activation increased across all areas in the activation pattern. Prefrontal activation was reported for very difficult tasks, suggesting that the frontal lobes may have been recruited for performing such difficult tasks. Certainly, more demanding eye movement tasks such as memory-guided saccades activate PFC (14, 15). If patients with pAD have overall reduced cognitive resources, particularly in the parietal lobes, as has been reported for spatial and object attention (1, 2, 5, 7), then even a normally simple reflexive task such as visually guided saccades may recruit resources from PFC. The asymmetry may reflect reduced cognitive resources for spatial attention in the right parietal lobe (7). The cognitively able elderly control volunteers show a pattern similar to that of young control volunteers, consistent with little loss of cognitive resources involved in eye movement control. The lack of correlation of activation patterns with the score of the mini-mental status examination is not surprising for these participants because this examination does not measure the cognitive processing of eye movement control or visuospatial processing in general.

Conclusion

This study shows that fMR imaging with the visually guided saccade paradigm can be successfully performed on both elderly cognitively able volunteers and patients with dementia. The fMR imaging activation pattern, showing a left-dominant LR for the IPS, has a high specificity, although lower sensitivity, for pAD. Considering that the clinical assessment has a lower specificity and requires a longer time, the fMR imaging study, performed in fewer than 10 minutes during the routine clinical MR examination, may be useful to improve the specificity of the clinical diagnosis. This result must be confirmed by further study, possibly across multiple institutions. The addition of another paradigm to probe memory function, which is the clinical hallmark of pAD, may increase the sensitivity of fMR imaging for diagnosis of pAD if a feasible paradigm can be designed for this patient population (34).

Acknowledgments

The authors acknowledge financial support from Public Health Service grants PO1 NS35949 and P50 AG05133 and from General Electric Medical Systems. Helpful discussions with Drs. Sweeney, DeKosky, Becker, and Lopez regarding the clinical evaluation of Alzheimer's disease are acknowledged.

References

1. Cronin-Golomb A, Corkin S, Rizzo JF, Cohen J, Growden JH, Banks KS. **Visual dysfunction in Alzheimer's disease: relation to normal aging.** *Ann Neurol* 1991;29:41–52
2. Cronin-Golomb A, Rizzo JF, Corkin S, Growdon JH. **Visual function in Alzheimer's disease and normal aging.** *Ann N Y Acad Sci* 1991;640:28–35
3. Mentis MJ, Horwitz B, Grady C, et al. **Visual cortical dysfunction in Alzheimer's disease evaluated with a temporally graded "stress test" during PET.** *Am J Psychiatry* 1996;153:32–40
4. Butter CM, Trobe JD, Foster NL, Berent S. **Visual–spatial deficits explain visual symptoms in Alzheimer's disease.** *Am J Ophthalmol* 1996;122:97–105
5. Mendez M, Cherrier MM, Cymerman JS. **Hemispatial neglect on visual search tasks in Alzheimer's disease.** *Neuropsychiatry Neuropsychol Behav Neurol* 1997;10:203–208
6. Stark ME, Grafman J, Fertig E. **A restricted "spotlight" of attention in visual object recognition.** *Neuropsychologia* 1997;35:1233–1249
7. Foster JK, Behrmann M, Stuss DT. **Aging and visual search: generalized cognitive slowing or selective deficits in attention?** *Aging and Cognition* 1995;2:279–300
8. Mielke R, Kessler J, Fink G, Herholz K, Heiss W. **Dysfunction of visual cortex contributes to disturbed processing of visual information in Alzheimer's disease.** *Int J Neurosci* 1995;82:1–9
9. Mesulam M-M. **A cortical network for directed attention and unilateral neglect.** *Ann Neurol* 1981;10:309–325
10. Weintraub S, Daffner KR, Ahern GL, Price BH, Mesulam M-M. **Right sided hemispatial neglect and bilateral cerebral lesions.** *J Neurol Neurosurg Psychiatry* 1966;60:342–344
11. Posner MI, Walker JA, Friedrich FJ, Rafal RD. **Effects of parietal injury on covert orienting of attention.** *J Neurosci* 1984;4:1863–1874
12. Coull JT, Nobre AC. **Where and when to pay attention: the neural systems for directing attention to spatial locations and to time intervals as revealed by both PET and fMRI.** *J Neurosci* 1998;18:7426–7435

13. McKann G, Drachman D, Folstein M, Katzman R, Price D, Stadlan EM. **Clinical diagnosis of Alzheimer's disease: report of the NINCDS-ADRDA work group under the auspices of Department of Health and Human Services task force on Alzheimer's disease.** *Neurology* 1984;34:939–944
14. Horwitz B, McIntosh AR, Haxby JV, et al. **Network analysis of PET-mapped visual pathways in Alzheimer's type dementia.** *Neuroreport* 1995;6:2287–2292
15. Thulborn KR, Davis D, Erb P, Strojwas M, Sweeney JA. **Clinical fMRI: Implementation and Experience.** *Neuroimage* 1996;4: S101–S107
16. Thulborn KR, Gillen JS, McCurtain B, Betancourt C, Sweeney JA. **Functional magnetic resonance imaging of the human brain.** *Bull Magn Reson* 1996;18:37–42
17. Thulborn KR, Voyvodic J, McCurtain B, et al. **High field functional MRI in humans: applications to cognitive function.** In: Pavolone P, Rossi P, eds. *Functional MRI*. Milan: Springer; 1996
18. Thulborn KR, McCurtain B, Voyvodic J, Chang S, Gillen J, Sweeney JA. **Functional MRI: the environment and technology for clinical application.** In: Pavone P, Rossi P, eds. *Functional MRI*. Rome: Springer; 1995:15–22
19. Thulborn KR, Talagala SL, Chang SY, et al. **High field clinical fMRI.** In: Scotti G, Le Bihan D, eds. *Syllabus of 6th Advanced Course of the European Society of Neuroradiology*. Bologna: Edizioni del Centauro; 1996:53–62
20. Thulborn KR, Voyvodic J, Chang S, Strojwas M, Sweeney JA. **New approaches to cognitive function by high field functional MRI.** In: Yuasa T, Prichard JW, Ogawa S, eds. *Current Progress in Functional Brain Mapping: Science and Applications.* London: Smith-Gordon;1998;15–24
21. Sweeney JA, Luna B, Strojwas M, et al. **Functional MRI studies of eye movement control: a paradigm for clinical applications.** *Proceedings of the Fifth Scientific Meeting of the International Society of Magnetic Resonance in Medicine.* Vancouver; 1997:451
22. Ogawa S, Tank DW, Menon RS, et al. **Intrinsic signal changes accompanying sensory stimulation: functional brain mapping using MRI.** *Proc Natl Acad Sci U S A* 1992;89:5951–5955
23. Kwong KK, Belliveau JW, Chesler DA, et al. **Dynamic magnetic resonance imaging of human brain activity during primary sensory stimulation.** *Proc Natl Acad Sci U S A* 1992;89: 5675–5679
24. Buck BH, Black SE, Behrmann M, et al. **Spatial- and object-based attentional deficits in Alzheimer's disease.** *Brain* 1997; 120:1229–1244
25. Binetti G, Cappa SF, Magni E, Padovani A, Bianchetti A, Trabucchi M. **Visual- and spatial perception in the early phase of Alzheimer's disease.** *Neuropsychology* 1998;12:29–33
26. Sweeney JA, Luna B, Strojwas MH, Thulborn KR. **Mapping distinct cortical eye fields for saccadic and pursuit eye movements in humans using fMRI.** *Proceedings of the 27th Annual Meeting of the Society of Neuroscience.* New Orleans;1997;864:8
27. Luna B, Thulborn KR, Strojwas MH, et al. **Dorsal cortical regions subserving visually guided saccades in humans: a fMRI study.** *Cereb Cortex* 1998;8:40–47
28. Eddy WF, Fitzgerald M, Noll DC. **Improved image registration by using Fourier interpolation.** *Magn Reson Med* 1996;36: 923–931
29. Cox RW. **AFNI: software for analysis and visualization of functional magnetic resonance neuroimages.** *Comput Biomed Res* 1996;29:162–173
30. Talairach J, Tournoux P. **Co-planar stereotaxic atlas of the human brain: 3D proportional system: an approach to cerebral imaging.** New York: Georg Thieme Verlag; 1988
31. Uttecht SD, Betancourt C, Thulborn KR. **Evaluation of semi-automated border recognition software for quantitative brain morphometry and topology from high-resolution MRI.** *Proceedings of the Sixth Scientific Meeting of the International Society of Magnetic Resonance in Medicine.* Sydney; 1998:2075
32. Just MA, Carpenter PA, Keller TA, Eddy WF, Thulborn KR. **Brain activation modulated by sentence comprehension.** *Science* 1996;274:114–116
33. Carpenter PA, Just MA, Keller T, Eddy W, Thulborn KR. **Graded functional activation in the visuo-spatial system with the amount of task demand.** *J Cogn Neurosci* 1999;11:9–24
34. Thulborn KR, Martin C, Sweeney JA. **Functional MRI with visually-guided saccades separates probable Alzheimer's disease from other dementias.** *Proceedings of the 28th Annual Meeting of the Society for Neuroscience.* Los Angeles;1998:1269